Ain Shams Engineering Journal 15 (2024) 102972

Contents lists available at ScienceDirect

Ain Shams Engineering Journal

journal homepage: https://www.sciencedirect.com

Full Length Article

Pilot point selection for secondary voltage control in active distribution networks with applications to an Australian feeder

Mubeenah Titilola Sanni [a], Hemanshu Roy Pota [a], Daoyi Dong [b], Huadong Mo [c,*]

[a] School of Engineering and Technology, The University of New South Wales, Canberra, 2600, Australia
[b] CIICADA Lab, School of Engineering, Australian National University, Canberra, ACT 2601, Australia
[c] School of Systems and Computing, The University of New South Wales, Canberra, 2600, Australia

ARTICLE INFO

Keywords:
Differential evolution
Distribution networks
Pilot point selection
Secondary voltage control

ABSTRACT

This paper presents a method for selecting pilot points used in secondary voltage control of active distribution networks. A unique formulation for pilot point selection is presented as a multi-objective stochastic optimization problem solved using differential evolution. The pilot point selection method considers multiple operating cases with different combinations of solar photovoltaic generation, loads, and electric vehicle uncertainties. The proposed methodology is applied to the IEEE 33 bus test system and a large Australian distribution feeder while observability, controllability, and robustness metrics are used to compare the proposed method against existing methods. Compared with the existing pilot point selection approaches, it is found that the proposed method obtains the most observable, controllable, and robust set of pilot points, making the method effective for the optimal selection of pilot points used in secondary voltage control of active distribution networks.

1. Introduction

Renewable energy sources are introduced in the power system grids to create cleaner and unlimited generation [1]. Intermittent renewable generation may cause voltage fluctuations and a change of direction in power flow [2–4]. These variations could result in voltage instability which could affect the security of the power system networks [5]. The capability of a power system to maintain steady voltages in the event of a disturbance or threat to the initial operating condition is known as voltage stability [6,7]. Bus voltages are allowed for a deviation of up to ±5 percent of the preset values for control purposes [8]. If the bus voltage values deviate further from this range, system instability may occur [9], requiring necessary control actions. Voltage profile control plays a vital role in ensuring the reliability of the power grid, security, and economical operation [10].

Voltage control can be achieved in power systems in a three-level hierarchy [11]. The first level is the primary voltage control which involves the management of generator buses by providing rapid responses to voltage variations using local feedback. A load bus where real-time voltage is measured for control actions is the pilot point. The second level is the Secondary Voltage Control (SVC), aiming to automatically correct pilot point voltages in the event of a bus voltage deviation in a given control area. It achieves this by managing the reactive power available in the area. The third level is the tertiary voltage control, which involves determining the optimal reference values of each pilot point in the grid [12].

An integral factor of a properly functioning SVC scheme is appropriate pilot point selection [13]. A properly selected pilot point should reflect the voltage variation in the control area [14]. The best location of pilot points should demonstrate the criteria of observability, controllability, and robustness [15]. Existing results have demonstrated that monitoring and controlling voltages at the pilot points maintain the voltage profile of the overall system [16–18].

Techniques for pilot point selection include selecting buses with the highest short circuit current or buses that have the capability to minimize voltage deviation after a random disturbance [19]. A method for pilot point selection based on the linearized model of the reactive power-voltage load flow equations was proposed in [20,21] using simulated annealing. Disturbances in the form of load loss and line losses were used to test and validate the obtained pilot points. According to [22], the method in [20] results in pilot points that are considered non-controllable because undervoltages and overvoltages were reported at

* Corresponding author at: Room 101, Building 20, School of Engineering and Information Technology, University of New South Wales, 2600, Australia.
E-mail addresses: m.sanni@student.unsw.edu.au (M.T. Sanni), h.pota@unsw.edu.au (H.R. Pota), Daoyi.Dong@anu.edu.au (D. Dong), huadong.mo@unsw.edu.au (H. Mo).

https://doi.org/10.1016/j.asej.2024.102972
Received 30 November 2022; Received in revised form 22 February 2024; Accepted 9 July 2024
Available online 18 July 2024

some load buses after the application of SVC. Another method was suggested in [11,23,24] to improve the controllability and obtain more controllable pilot points. An electrical distance that represents the controllability of pilot points to load buses was proposed in [11] and a much-improved voltage profile after applying the controllers on the pilot points was observed. The system modeling for pilot point selection relies on the voltage and reactive power changes caused by disturbances. In [25], uncertainties in the form of load and topology were introduced in the modeling to improve the robustness of obtained pilot points against disturbances. A probabilistic determination approach, solved by the immune algorithm, was proposed in [26] to determine robust pilot points. The obtained results demonstrated improved voltage profiles when controllers were placed at the selected pilot points. To ensure the criteria of observability, controllability, and robustness are satisfied, a multi-objective probabilistic model was introduced in [27], and it was solved using the non-dominated sorting genetic algorithm and fuzzy (NSGA-II). However, all these methods were proposed for the transmission network and a clear justification for the number of pilot points required was not provided.

Transmission and distribution networks have different characteristics, primarily in terms of R/X ratios. Furthermore, high penetration of distributed generation [28–30] converts the traditional distribution network that typically has a single source of energy injection to an active distribution network with multiple sources of energy injections primarily via roof-top solar photovoltaics (PVs). The control techniques available for the distribution network include the droop technique which has been proven to be insufficient in [31,32]. Another technique involves simply selecting buses with critical loads or buses at the end of the feeder as pilot points. These points do not guarantee the observability of the whole network but a pilot point voltage should serve as a representative of other load bus voltages in the control area. The points selected via this approach are also not controllable as the pilot point should be highly sensitive to generator control actions.

The major contribution of this paper is providing a robust pilot point selection methodology using Multi-Objective Differential Evolution (MODE) with applications to a real Australian distribution feeder. To our best knowledge, the control effect of pilot points on active distribution networks (ADNs) is yet to be explored, which is neglected by existing studies. The method proposed is simple, efficient, and effective, and produces pilot points that are observable, controllable, and robust. The robustness of the pilot points is achieved through modeling uncertainties related to load, PVs and electric vehicles (EVs) using the approach of probabilistic determination. In addition, comprehensive simulation studies are conducted to demonstrate that the proposed method gives better observable, controllable, and robust pilot points compared to existing approaches.

The remainder of the paper is structured as follows. Section 2 presents the mathematical modeling formulation. Section 3 presents the pilot point selection method, while Section 4 discusses the results, and the conclusions are presented in Section 5.

2. Mathematical modeling

Consider a distribution network consisting of n generator buses and m load buses. For $I = \{1, 2, ..., n+m+1\}$, the power flow equations can be given as follows [33]:

$$\begin{cases} P_i = P_{Gi} - P_{Li} = V_i \sum_{j\epsilon I} V_j \left(G_{ij}\cos\theta_{ij} + B_{ij}\sin\theta_{ij}\right) \\ Q_i = Q_{Gi} - Q_{Li} = V_i \sum_{j\epsilon I} V_j \left(G_{ij}\sin\theta_{ij} - B_{ij}\cos\theta_{ij}\right) \\ i = 1, 2, ..., n+m+1 \end{cases} \tag{1}$$

where P_i and Q_i are the active and reactive power injections at buses i, respectively, V_i and V_j are the voltage magnitudes at buses i and j, $(\theta_{ij} = \theta_i - \theta_j)$ is the difference in phase angle between the ith and jth buses, G_{ij} and B_{ij} are the real and imaginary parts of the elements in the bus admittance matrix $(Y_{ij} = G_{ij} + jB_{ij})$ corresponding to the ith row and jth column.

Let $V_i^0, \theta_i^0, P_i^0, Q_i^0$ denote the equilibrium points, and the variations in voltage magnitudes and angles at the ith bus can be defined as $\Delta V_i = V_i - V_i^0$ and $\Delta\theta_i = \theta_i - \theta_i^0$. The changes in active and reactive power injections are defined as $\Delta P_i = P_i - P_i^0$ and $\Delta Q_i = Q_i - Q_i^0$. Vectors $\Delta V = [\Delta V_1, \Delta V_2, \ldots, \Delta V_{n+m}]^T$ and $\Delta\theta = [\Delta\theta_1, \Delta\theta_2, \ldots, \Delta\theta_{n+m}]^T$ represent the vectors of the change in bus voltage magnitudes and angles while vectors $\Delta P = [\Delta P_1, \Delta P_2, \ldots, \Delta P_{n+m}]^T$ and $\Delta Q = [\Delta Q_1, \Delta Q_2, \ldots, \Delta Q_{n+m}]^T$ are the vectors of the change in bus active and reactive power. The linearized form of (1) around the equilibrium point can be written as:

$$\begin{bmatrix} \Delta P \\ \Delta Q \end{bmatrix} = \begin{bmatrix} B & H \\ L & S \end{bmatrix} \begin{bmatrix} \Delta\theta \\ \Delta V \end{bmatrix} \tag{2}$$

where $B = B(i,j) = \left[\frac{\partial P_i}{\partial \theta_j}\right]$, $H = H(i,j) = \left[\frac{\partial P_i}{\partial V_j}\right]$, $L = L(i,j) = \left[\frac{\partial Q_i}{\partial \theta_j}\right]$, and $S = S(i,j) = \left[\frac{\partial Q_i}{\partial V_j}\right]$. The sensitivity of ΔV to ΔQ is utilized for pilot point selection and it is formulated using the decoupled power flow model of the linearized steady-state equations and can be represented as:

$$\begin{bmatrix} \Delta Q_{G1} \\ . \\ . \\ \Delta Q_{Gn} \\ \Delta Q_{L1} \\ . \\ . \\ \Delta Q_{Lm} \end{bmatrix} = \begin{bmatrix} S_{GG} & S_{GL} \\ S_{LG} & S_{LL} \end{bmatrix} \begin{bmatrix} \Delta V_{G1} \\ . \\ . \\ \Delta V_{Gn} \\ \Delta V_{L1} \\ . \\ . \\ \Delta V_{Lm} \end{bmatrix} \tag{3}$$

where S_{GG} is a $n \times n$ matrix with $S_{GG}(i,j) = \left[\frac{\partial Q_{Gi}}{\partial V_{Gj}}\right]$,

S_{GL} is a $n \times m$ matrix with $S_{GL}(i,j) = \left[\frac{\partial Q_{Li}}{\partial V_{Gj}}\right]$,

S_{LG} is a $m \times n$ matrix with $S_{LG}(i,j) = \left[\frac{\partial Q_{Gi}}{\partial V_{Lj}}\right]$,

S_{LL} is a $m \times m$ matrix with $S_{LL}(i,j) = \left[\frac{\partial Q_{Li}}{\partial V_{Lj}}\right]$;

$\Delta Q_G = [\Delta Q_{G1}, ..., \Delta Q_{Gn}]^T$ represents the vector of injected reactive power changes;

$\Delta Q_L = [\Delta Q_{L1}, ..., \Delta Q_{Lm}]^T$ denotes the vector of the disturbance caused by reactive fluctuations of the load buses;

$\Delta V_G = [\Delta V_{G1}, ..., \Delta V_{Gn}]^T$ denotes the vector of voltage magnitude changes of the generator buses;

$\Delta V_L = [\Delta V_{L1}, ..., \Delta V_{Lm}]^T$ denotes the vector of voltage magnitude changes of load buses.

Vector ΔV_L represents the vector of the load bus voltage deviations, and this can be obtained from (3) as follows:

$$\Delta V_L = S_{LL}^{-1}\Delta Q_L - S_{LL}^{-1}S_{LG}\Delta V_G. \tag{4}$$

A pilot point selection matrix A is defined as:

$$\Delta V_A = A\Delta V_L \tag{5}$$

where A is an $n_A \times n_L$ matrix with binary elements. n_A and n_L denote the numbers of pilot points and load buses, respectively. A_{ij} can be defined as

$$A_{ij} = \begin{cases} 1, & \text{should bus } j \text{ be the } i\text{th pilot point} \\ 0, & \text{otherwise} \end{cases} \tag{6}$$

Substituting (4) in (5) results in a vector of pilot point voltage deviation as follows:

$$\Delta V_A = AS_{LL}^{-1}\Delta Q_L - AS_{LL}^{-1}S_{LG}\Delta V_G. \tag{7}$$

The aim is to maintain zero voltage deviation at the selected pilot points using minimum reactive power compensation [34]. This would, in turn, keep the voltage levels at other load buses in the network within the limit, i.e.,

$$\Delta V_A = F\Delta Q_L + M\Delta V_G = 0 \tag{8}$$

where the introduced matrices are defined as follows:

$$F = AS_{LL}^{-1}, \tag{9}$$

$$M = -AS_{LL}^{-1}S_{LG}. \tag{10}$$

From (8), the change in reactive power of the generators ΔV_G which is needed to counteract the effect of the disturbances ΔQ_L is given by:

$$\Delta V_G = -BM^{-1}F\Delta Q_L. \tag{11}$$

B represents the optimal feedback gain matrix to enforce the change in voltage at pilot points ΔV_A to zero through minimizing the norm of ΔV_G, $||\Delta V_G||_2$. The pilot point selection problem seeks to find a subset of pilot points among the set of load buses that minimizes ΔV_L. Replacing the ΔV_G term of (4) with (11) gives:

$$\Delta V_L = (I - MBA)F\Delta Q_L. \tag{12}$$

3. Pilot point selection

Choosing pilot points among load buses in a power system network is a complex problem that can be solved effectively by heuristic algorithms [23]. In this paper, MODE, a stochastic population-based algorithm, is used to optimize the pilot points selection. MODE has advantages, including obtaining optimal solutions irrespective of the initial parameters, being computationally simple, and robust, and having the ability to handle integer and discrete optimization with a fast convergence rate [35]. MODE can outperform GA, PSO [35], and simulated annealing [36] in terms of convergence speed and selecting the lowest fitness function for the problems considered.

3.1. Objective functions

The objective of the pilot point selection problem is to determine the locations of the pilot points which satisfy the criteria of observability, controllability, and robustness. To satisfy the three criteria, three objectives are developed. The first objective aims at producing robust pilot points capable of minimizing the absolute voltage deviation at all load buses. Furthermore, an uncertainty index is added to the first objective to model load and generation uncertainties as follows:

$$G_1 = F_1 = \sum_{j=1}^{s} \rho_j (\Delta V_{L,j}^T Z_x \Delta V_{L,j}) \tag{13}$$

where s is the number of scenarios considered, ρ_j is the probability of the jth scenario, $\Delta V_{L,j}$ denotes the voltage magnitude changes of load buses at scenario j, and Z_x refers to a diagonal weighting matrix needed to place priority on the importance of load buses to meet the additional voltage control requirements.

The second objective aims at maximizing the voltage sensitivity among load buses to ensure that the load buses with the largest sensitivities to other load buses are chosen as the pilot points thereby ensuring observability is maximized:

$$G_2 = -F_2 = -\sum_{i=1}^{n_A}\sum_{j=1,j\neq i}^{n_L}\sqrt{\left(\frac{S_{LL}(i,j)}{S_{LL}(j,j)}\right)^2 + \left(\frac{S_{LL}(j,i)}{S_{LL}(j,j)}\right)^2}. \tag{14}$$

The third objective aims at maximizing the sensitivity of the load bus voltages to the generator bus voltages to ensure the load buses with the highest sensitivities to the generators are selected as pilot points (controllability). This can be expressed as:

$$G_3 = -F_3 = -\sum_{i=1}^{n_A}\sum_{j=1,j\neq i}^{n_G}\sqrt{\left(\frac{S_{LL}(i,j)}{S_{LL}(j,j)}\right)^2 + \left(\frac{S_{LL}(j,i)}{S_{LL}(j,j)}\right)^2} \tag{15}$$

where n_G is the set of generator buses. The proposed multi-objective formulation is expressed as:

$$\min_A \{G_1, G_2, G_3\} \tag{16}$$

where A represents the pilot point selection matrix.

3.2. Multi-objective differential evolution

DE is an evolutionary optimization algorithm whose optimization variables may be represented with floating-point numbers in the population [37]. The algorithm begins by randomly choosing the initial candidate solutions while exploring the boundary of the search space. New offspring are generated by creating noisy replicas of the individuals in the population. DE is extended in this paper to solve the proposed objective functions. To select the best compromise solution from all the solutions that satisfy the different objectives, a technique based on fuzzy set theory is introduced to assign a membership function to each objective function used. The linear membership for each objective function G_i in the solution is defined as follows:

$$\mu = \begin{cases} 1, & G_i \geq G_i^{max} \\ \frac{G_i^{max} - G_i}{G_i^{max} - G_i^{min}}, & G_i^{min} < G_i < G_i^{max} \\ 0, & G_i \leq G_i^{min} \end{cases} \tag{17}$$

where G_i^{min} and G_i^{max} are the lower and upper limits of the i^{th} solution to the objective functions. The membership function for the solutions in a fuzzy set can be calculated as follows:

$$\mu^j = \frac{\sum_{i=1}^{M_{obj}} \mu_i^j}{\sum_{k=1}^{W}\sum_{i=1}^{M_{obj}} \mu_i^j} \tag{18}$$

where W are the number of solutions and M_{obj} is the number of objectives. The solution with the maximum membership function is the best compromise solution.

3.3. Scenario modeling

Choosing pilot points is performed only once, and then used to implement a secondary voltage control scheme. Since the selection is done once, it is essential to consider different representative operating scenarios relevant to the system. An efficient tool used in dealing with unknown parameters and uncertainties is stochastic programming. The most common stochastic programming approaches are the chance-constrained method, scenario-based method, and the expected value method [38]. The expected value method replaces the input data with respected expected values [38] while the chance-constrained method considers the possibility of constraint violations as probabilities resulting in a computationally intractable problem since it requires the computation of multi-dimensional probability integrals [39]. Nevertheless, both approaches result in a deterministic optimization problem that considers only the worst-case scenario. Obtaining the worst-case scenario is not always possible leading to a solution that once implemented may not be the best outcome [40].

The pilot point selection problem is modeled as a scenario-based stochastic problem due to its efficiency and computational tractability. The scenario-based method employs occurrence probabilities to approximate the input data. The selected pilot nodes are expected to be robust against changing load demand and PV generation uncertainties. The load of a power system network can be categorized based on consumer demand. The demand levels can be determined by utilizing a suitable clustering algorithm. The k-means centroid clustering is used in this paper based on the study performed in [41] where it demonstrated better

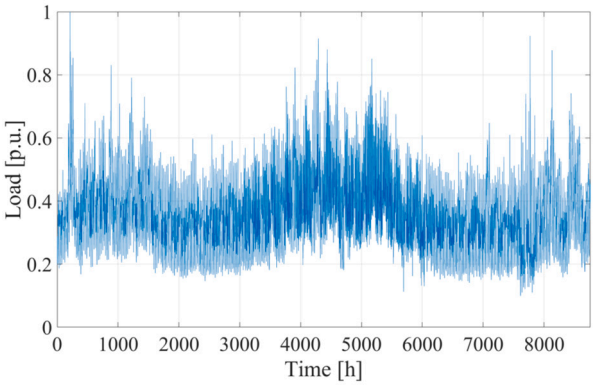

Fig. 1. Hourly demand profile.

Table 1
Load levels and their probabilities.

ID	Load Level	Probability
1	0.1824	0.0881
2	0.2290	0.1015
3	0.2730	0.1379
4	0.3142	0.1564
5	0.3591	0.1376
6	0.4056	0.1194
7	0.4612	0.1155
8	0.5289	0.0800
9	0.6185	0.0529
10	0.7658	0.0107

performance on an application to a reduced model of a European feeder. The k-means clustering technique divides the input dataset, and the load demand profile into a specified number of clusters and returns a set of seeds representing each cluster's centroids and a vector of probabilities associated with each cluster. The distribution system used follows the hourly demand profiles of 114 households [42]. Furthermore, to take into account the increasing penetration of electric vehicles [43], 20 households have been equipped with electric vehicle charging stations and their charging profiles have been added to the hourly demand profiles of the households. The hourly demand profile of the distribution system for a year as seen at the substation level is shown in Fig. 1 [42]. By performing the nearest centroid clustering, 10 equivalent clusters have been obtained from the hourly demand profile. The ten levels of load demand and their associated probabilities are given in Table 1. Fig. 2 also shows the sorted load demand profile with different colors representing separate clusters.

To take into account the generation diversity of PV systems, the same centroid clustering technique is applied to the hourly irradiance profiles obtained for Canberra from January 2018 to January 2021 [42]. The direct normal irradiance which represents the dominant irradiance component when performing solar generation studies along with the clustered dataset is shown in Fig. 3 and Fig. 4. The PV generation corresponding to each cluster and their associated probabilities associated are given in Table 2.

The ten load and PV generation levels obtained would yield 100 test scenarios that would raise the computational intensity of the optimization task. It is necessary to reduce the number of scenarios by adopting a scenario-reduction technique. Scenario reduction aims to select a set from the original set of scenarios that serve as a trade-off between lower computational burden and information loss [44]. Scenario reduction algorithms in the literature include backward reduction, simultaneous backward reduction, and fast-forward selection [45]. An optimal algorithm reduces the number of scenarios but retains most of the information in the original set of scenarios. Comparisons among the three algorithms were made in [45] and their results indicate the

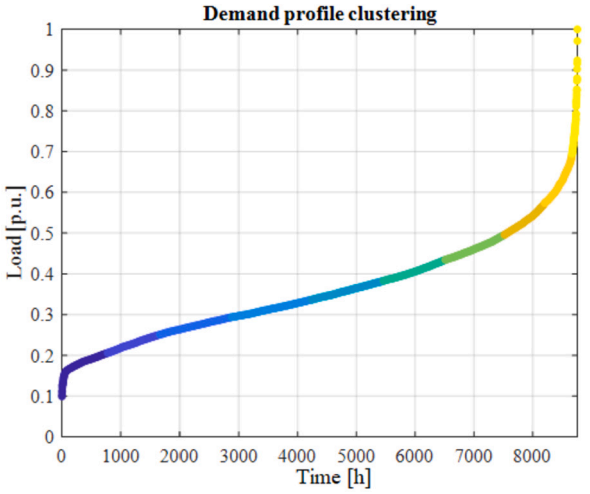

Fig. 2. Clustered demand profile.

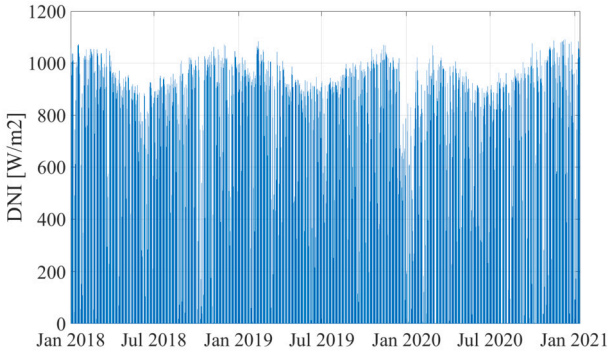

Fig. 3. Hourly direct normal irradiance profile: Canberra, 2018-2021.

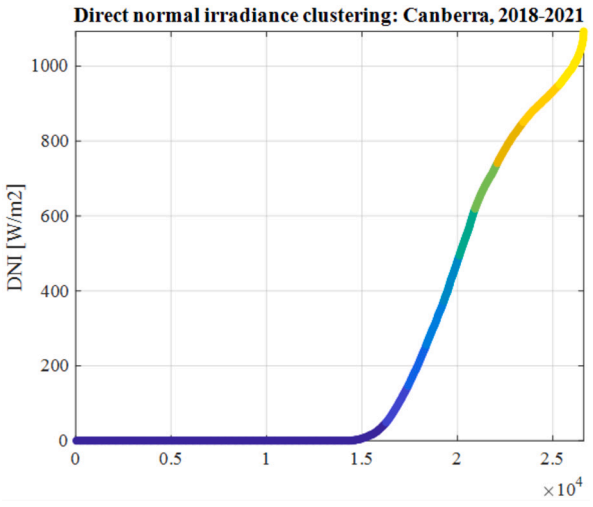

Fig. 4. Clustered direct normal irradiance.

fast-forward selection to be faster, optimal, and the most accurate. The number of reduced scenarios that will guarantee optimal performance is chosen in this paper as that in which the *Kantorovich distance* [40] between the original and reduced sets of scenarios is minimal. Based on this distance, 20 scenarios are chosen to guarantee optimal performance. Table 3 features the list of reduced scenarios obtained using this technique and the associated probabilities.

After scenario generation, the control generators are selected as the solar PV locations with abundant effective reactive power reserves. The

Table 2
Photo-voltaic generation levels and their probabilities.

ID	PV generation	Probability
1	0.0016	0.6104
2	0.0855	0.0435
3	0.1820	0.0361
4	0.2871	0.0345
5	0.3959	0.0302
6	0.5075	0.0307
7	0.6248	0.0436
8	0.7312	0.0509
9	0.8251	0.0706
10	0.9141	0.0494

Table 3
Reduced states and their probabilities.

ID	Load level	PV generation	Probability
1	0.7658	0.3959	0.0003
2	0.7658	0.5075	0.0003
3	0.7658	0.2871	0.0004
4	0.7658	0.1820	0.0004
5	0.7658	0.6248	0.0005
6	0.7658	0.0855	0.0393
7	0.7658	0.7312	0.0005
8	0.7658	0.9141	0.0128
9	0.7658	0.8251	0.0045
10	0.6185	0.3959	0.0016
11	0.6185	0.5075	0.0016
12	0.6185	0.2871	0.0018
13	0.5289	0.3959	0.0095
14	0.5289	0.5075	0.0301
15	0.6185	0.1820	0.3925
16	0.1824	0.3959	0.0665
17	0.1824	0.5075	0.1110
18	0.6185	0.6248	0.0839
19	0.5289	0.2871	0.1213
20	0.2290	0.3959	0.1211

final step is to implement the optimization algorithm using the objective functions to obtain the optimal pilot points.

4. Result and discussion

The method presented in this paper is tested on the IEEE 33 node test feeder depicted in Fig. 5. The technical data of the network is given in [46]. The disturbance variables ΔQ_L are modeled by a Gaussian variable vector whose average is zero and its standard deviation is proportional to the load reactive power at an operation condition [11].

4.1. Optimal selection of pilot points

In order to accurately determine the number of pilot points that leads to sufficiently accurate voltage control, 15,000 scenarios have been considered in the case of the IEEE 33-node test feeder. The number of pilot points is varied from 1 to 15 and 1,000 scenarios of pilot points in each simulation are considered. The box plot of the obtained results is shown in Fig. 8. The horizontal axis corresponds to the number of pilot points and the vertical axis corresponds to the performance index (PI). PI is calculated as:

$$PI = \sum_{j=1}^{s} \rho_j \text{ trace } (|V_{L,i}|). \tag{19}$$

PI depends on the chosen set of pilot points and the optimal pilot point set yields the PI. The whiskers extend to the most extreme data points (outliers) and are plotted individually using the '+' marker symbol. It is observed that at least 5 pilot points are needed to establish a feasible voltage control. The minimal PI which corresponds with the optimal pilot point selection scenarios does not change drastically after the number of pilot points reaches 7. Though increasing the number of pilot points leads to a lower mean voltage deviation, further increasing the number of pilot points is costly, since the pilot points need to be covered with voltage measurement units. Therefore, seven pilot points are chosen as optimal in the case of the IEEE 33 bus radial distribution system. Using seven pilot points, the voltage deviation at all load buses is obtained and depicted in Fig. 7. The voltage profile of the network for all the nodes with the proposed technique with respect to the optimal power flow of the network is shown in Fig. 6. It can be clearly seen that the voltage profile of the network with the proposed technique has a smaller voltage deviation for certain buses compared to that without the proposed technique.

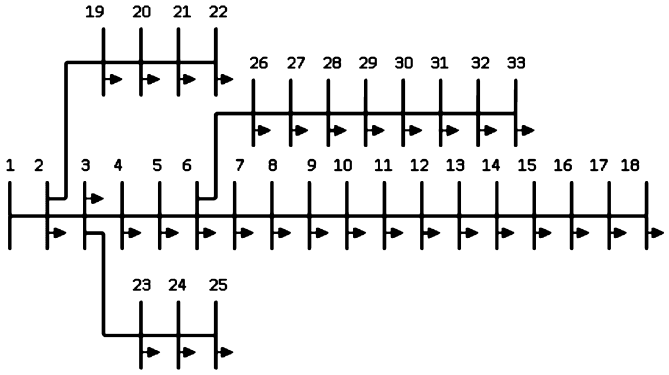

Fig. 5. IEEE 33 bus test system.

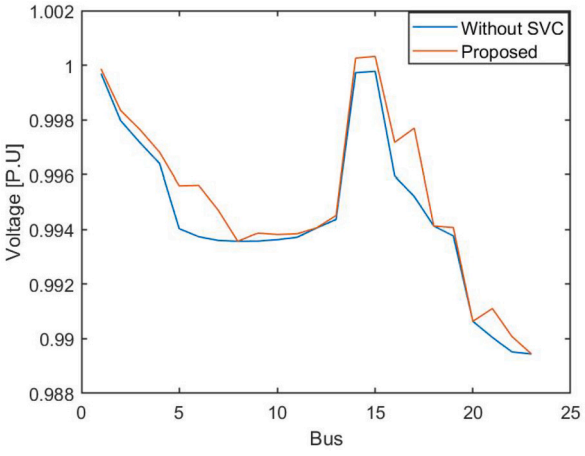

Fig. 6. Voltage profile with and without pilot point selection.

The numerical results for different numbers of pilot points are outlined in Table 4. The table shows the mean bus voltage deviation for the twenty analyzed scenarios for the chosen set of pilot points. The values are obtained by running the optimization algorithm for different numbers of pilot points. As can be seen, the maximum voltage deviation resulting from the reactive power disturbance in the analyzed scenarios is well below $0.05p.u$ which is a negligible error for practical implementations [8].

Another set of pilot points is selected by fixing the first five points and searching for varying numbers of points. The five points selected represent the most connected nodes in the system. This analysis is done to investigate the possibility of obtaining a lower voltage deviation if well-connected nodes are selected as the starting point. An alternate reason for this analysis is to factor in the increasing complexity of the modern distribution system. With more nodes added to the base distribution system, extra pilot nodes can be added while fixing the original set of pilot points. The obtained result depicted in Table 5 shows a similar trend as in Table 4 with an increasing number of pilot points. However, the

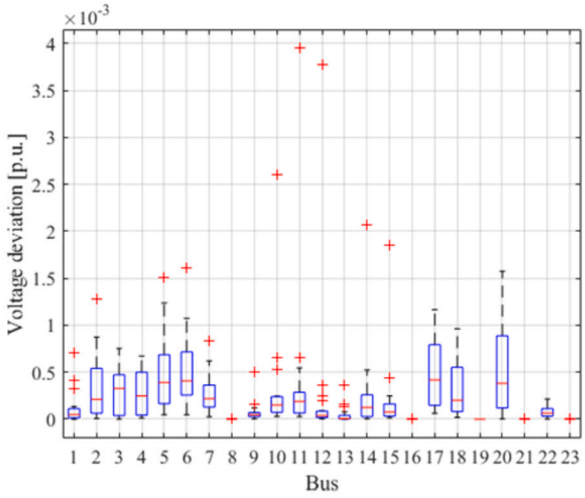

Fig. 7. Box plot of load bus voltage deviation for the optimal pilot points set.

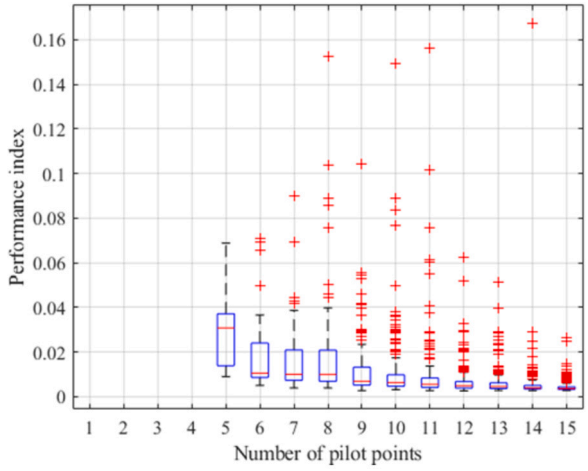

Fig. 8. Performance of different numbers of pilot points.

Table 4
Fitness values for different sets of pilot points.

n_A	Pilot points	Minimum PI
5	3, 13, 17, 21, 32	0.0102
6	7, 9, 17, 20, 24, 32	0.0063
7	2, 13, 17, 20, 26, 30, 31	0.0047
8	2, 7, 8, 17, 21, 24, 29, 31	0.0039
9	29, 20, 17, 31, 3, 26, 24, 12, 13	0.0032
10	31, 2, 29, 17, 26, 10, 3, 21, 24, 13	0.0027

Table 5
Fitness values for alternate sets of pilot points.

n_A	Pilot points	Minimum PI
5	5, 9, 16, 20, 30	0.0113
6	5, 9, 16, 20, 30, 32	0.0065
7	5, 9, 16, 20, 30, 32, 26	0.0052
8	5, 9, 16, 20, 30, 32, 26, 29	0.0041
9	5, 9, 16, 20, 30, 32, 26, 29, 21	0.0035
10	5, 9, 16, 20, 30, 32, 26, 29, 21, 24	0.0029

value of the objective function is slightly higher than when the algorithm searched for all the points. Furthermore, the 7 pilot points obtained are observed to be distributed throughout the entire feeder, and this is expected to achieve optimal control.

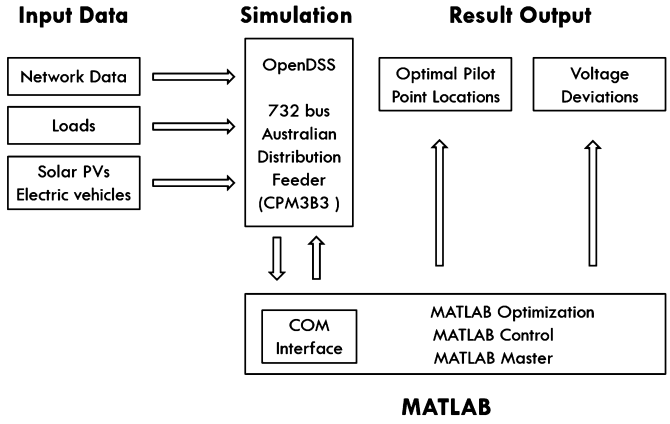

Fig. 9. Block diagram of the implemented procedure.

4.2. Application to an Australian feeder

The proposed approach is applied to a 732-bus distribution feeder located in New South Wales, Australia to validate the performance of an unbalanced large real-life system. The feeder consists of 966 loads and 715 lines with single, double and three-phase split circuits yielding a total of 2010 node points. The feeder is WYE configured, which has 19 transformers and operates at a nominal voltage of 11 kV. It is characterized by unbalanced loading and a single regulator at the substation. The feeder has a total load demand of 3282.9 kW and 469.5 kvar.

The overall algorithm is implemented in MATLAB and is based on two-way data exchange between the MATLAB code, which evaluates the optimization and assesses the control variable variations, and the OpenDSS simulation engine which performs the load flow and implements control variable variations on the network model. This data exchange is performed by means of a Component Object Model (COM) interface that is available in the OpenDSS package [47] and MATLAB uses the built-in ActiveX server to communicate with the COM Server of the OpenDSS. Any other distributed load flow software (research or industrial grade) can be exploited, provided that it is fast and reliable and has an easy data exchange interface. This procedure is depicted in Fig. 9.

The first step is to interface the PVs on random buses using real dispatch curves. Afterward, the load flow is performed and the voltage magnitudes in *p.u.* for all nodes of the three phases are obtained. Then each load is extracted and the buses are noted where it is connected (it can be a single phase, two phases, or three phases). Since this will form a repetition for the two and three-phase loads, the unique buses are obtained and denoted as the load buses from which the pilot nodes would be selected. Then a single sensitivity matrix is calculated using [48]. To determine the optimal number of pilot points, 10,000 scenarios have been considered, where the number of pilot points is varied from 10 to 100 and 1,000 scenarios of pilot points in each simulation are considered, without introducing uncertain load and solar photovoltaic.

The boxplot depicting the performance of different numbers of pilot points is shown in Fig. 10. Thirty pilot points are needed to establish a feasible voltage control as a lesser number of pilot points does not fulfill the observability criteria. As a result, the optimization does not converge for less than thirty pilot points. At 80 points, the change in PI is considered not significant, and hence 80 pilot points are considered optimal for the Australian feeder. Finally, the average bus voltage deviation for different numbers of pilot points for the twenty analyzed scenarios is shown in Table 6. It can be observed that the mean voltage deviation for all the load buses is less than 0.05 at 80 pilot points. Similar to the IEEE 33 feeder, the optimal pilot points selected by the proposed method are observed to be distributed throughout the entire feeder, and this is expected to achieve optimal control.

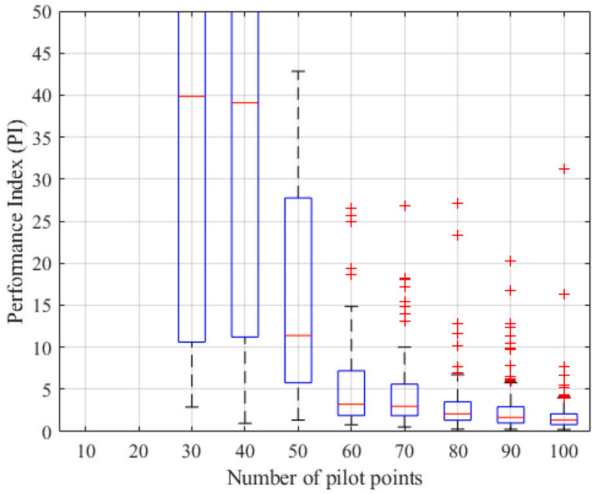

Fig. 10. Performance of different numbers of pilot points.

Table 6
Voltage deviation for different sets of pilot points.

n_A	Voltage deviation	
	Mean	Maximum
30	2.1	5.955
40	0.242	0.54
50	0.133	0.4
60	0.064	0.117
70	0.0451	0.081
80	0.0416	0.071
90	0.0096	0.069
100	0.0253	0.057

4.3. Quantification of observability, controllability and robustness

The proposed pilot point selection method is compared in this section with other pilot point selection methods using the observability, controllability and robustness metrics.

4.3.1. Observability

An observable pilot point is a bus whose voltage is highly sensitive to the voltage variations at the rest of the load buses [27]. This implies that the voltage changes at other load buses in the network would be observed at the pilot point. Hence, the knowledge of the pilot point voltages may be enough to serve as a control input for the voltage regulation of the whole network. The observability of a pilot point can be quantitatively characterized as follows: for a given reactive load disturbance ΔQ_l, pilot points must make the voltage deviation minimal. To quantitatively characterize the observability, a small reactive disturbance of ΔQ_L is applied on the load buses of the system. Then, load flow is performed to obtain a matrix γ which relates the change in voltage of the pilot point with respect to the other load bus in the network. The matrix γ spans $n_P \times n_L$ matrix. For y pilot points and z load buses:

$$\gamma = \begin{bmatrix} \frac{\delta V_{P1}}{\delta V_{J1}} & \frac{\delta V_{P1}}{\delta V_{J2}} & \cdots & \frac{\delta V_{P1}}{\delta V_{Jz}} \\ \vdots & \vdots & \cdots & \vdots \\ \frac{\delta V_{Py}}{\delta V_{J1}} & \frac{\delta V_{Py}}{\delta V_{J2}} & \cdots & \frac{\delta V_{Py}}{\delta V_{Jz}} \end{bmatrix}. \tag{20}$$

A similar matrix γ^* is generated by obtaining pilot points using techniques proposed in [20,24,26,27] and the application of a slight reactive disturbance:

$$\gamma^* = \begin{bmatrix} \frac{\delta V_{L1}}{\delta V_{J1}} & \frac{\delta V_{L1}}{\delta V_{J2}} & \cdots & \frac{\delta V_{L1}}{\delta V_{Jz}} \\ \vdots & \vdots & \cdots & \vdots \\ \frac{\delta V_{Ly}}{\delta V_{J1}} & \frac{\delta V_{L7}}{\delta V_{J2}} & \cdots & \frac{\delta V_{L7}}{\delta V_{J23}} \end{bmatrix}. \tag{21}$$

To compare the two matrices, the Frobenius norm, which is defined as the square root of the sum of the absolute squares of its elements is computed. The Frobenius norm computes the size of a matrix in scalar terms to allow for easy comparison. For an $m \times n$ matrix A, the Frobenius norm is defined as:

$$||A||_F \equiv \sqrt{\sum_{i=1}^{m}\sum_{j=1}^{n}|A_{ij}|^2}. \tag{22}$$

It is observed from the first column of Table 7 that $||\gamma||_F$ of the proposed pilot point selection method is higher than the values of the existing methods. This translates to a higher voltage coupling of the load buses to the proposed pilot points compared to the pilot points obtained from other techniques. Thus the obtained result shows that the proposed method gives the most observable load buses as pilot points.

4.3.2. Controllability

A controllable pilot point is a bus that is highly sensitive to generator control actions. This allows pilot points to maintain their voltage profile after a disturbance through the reactive power contribution of the PVs. To quantify controllability, an index β, which measures the deviation of the pilot points is proposed:

$$\beta = \sum_{i=1}^{n_A}|V_{pi} - V_{poi}| \tag{23}$$

where V_{pi} and V_{poi} are the voltage magnitudes of the pilot points i with and without disturbance, respectively. The metric β is obtained and the values are depicted in the third column of Table 7. From (8), the ideal set of pilot points should produce the value of β closest to zero. A value close to zero means that pilot points are maintained at a value equal to or close to the reference value. It can be observed from Table 7 that the proposed method obtains the most controllable pilot points in the system.

4.3.3. Robustness

The scenarios considered capture the extreme ends and the midpoints of the load and PV curve graph thus representing different possible operating conditions of a power system. This allows the obtained pilot points to provide voltage control with minimal voltage deviation irrespective of the operating condition of the system. Thus, a metric α which measures the absolute voltage deviation denoted in (24) is used to quantify the robustness of the pilot points:

$$\alpha = \frac{1}{n_L}\sum_{i=1}^{n_L}(|V^*| - |V|), \tag{24}$$

where $|V^*|$ and $|V|$ are voltage magnitudes of the load buses after and before disturbance, respectively. A lower value of absolute voltage deviation indicates a better choice of pilot points. To demonstrate the robustness of the pilot points obtained, the value of α is obtained. These values are displayed in Table 8 for all the 20 scenarios considered, representing the load and solar photovoltaic disturbances introduced in the simulation to evaluate the robustness. The proposed method has the best robustness evidenced by the smallest value of α. A summary of the comparison metrics of observability, controllability, and robustness is displayed in Table 7, where it is observed that the proposed method demonstrates the best results, i.e., the highest value of observability defined by (22) - highest voltage coupling of the load buses to the proposed pilot points, the lowest value of controllability defined by (23) – best maintaining the pilot points at a value equal to or close to the refer-

Table 7
Performance comparison.

Solution method	Observability	Controllability	Robustness	Computation time (min)
[20]	27.7416	0.0563	0.00364	7
[24]	34.6031	0.0257	0.00228	5
[27]	33.1789	0.0423	0.00200	4
[26]	44.2452	0.0285	0.00196	5
[49]	26.1728	0.0257	0.00187	4
Proposed	51.8656	0.0212	0.00183	3

Table 8
Mean voltage deviation for the 20 scenarios.

Scenario	Average voltage deviation [10^{-3} P.U]					
	[20]	[24]	[27]	[26]	[49]	Proposed
1	7.35	1.77	0.96	1.60	1.21	1.61
2	2.75	2.33	2.73	2.10	1.81	3.07
3	1.51	0.85	1.30	0.88	1.24	0.88
4	7.34	1.56	0.21	1.71	0.80	1.01
5	3.25	2.60	3.98	1.45	3.28	1.95
6	2.20	1.24	4.22	1.29	3.9	1.55
7	4.38	3.30	2.21	3.05	2.19	3.67
8	5.05	4.29	0.01	4.27	2.23	2.58
9	6.38	4.36	0.72	3.84	0.24	4.89
10	2.59	7.22	2.85	6.21	1.29	1.95
11	2.35	1.30	3.86	1.30	1.33	1.52
12	13.0	2.16	2.58	1.79	2.44	1.98
13	1.13	0.57	0.30	0.52	0.06	0.56
14	3.77	2.30	1.34	2.04	2.95	2.01
15	2.56	1.42	0.81	1.35	0.71	1.90
16	0.89	0.70	0.00	0.74	0.98	0.62
17	0.51	0.48	4.82	0.57	5.40	0.53
18	2.35	2.69	3.47	1.39	3.63	1.41
19	2.07	2.62	3.40	2.01	1.55	1.66
20	1.10	1.77	0.00	0.99	0.04	1.22

ence value, and the lowest value of robustness defined by (24) – best minimizing the absolute voltage deviation after and before disturbance.

5. Conclusion

This paper has presented a method to select pilot points for SVC. The proposed method was tested on the IEEE 33 and a real test feeder in Australia and metrics to quantify observability, controllability, and robustness have been developed. The results were analyzed in comparison with existing approaches. It was found that the method proposed in this paper improves the previous approaches in three respects: it considers the effects of different operating conditions regarding uncertainties in load including EV loads and PV generation forecast, provides the best performance for the observability, controllability, and robustness quantification and it is applicable to real distribution network applications. It can be concluded that the proposed method is applicable to large distribution feeders. In addition, the pilot points obtained from the proposed method demonstrate better observability, controllability, and robustness and are more suitable to be used in SVC. Future work would be focused on assigning small home roof PV inverters to these pilot points for SVC implementation.

Declaration of competing interest

The authors declare that they have no known competing financial interests or personal relationships that could have appeared to influence the work reported in this paper.

References

[1] Yu X, Xue Y. Smart grids: a cyber–physical systems perspective. Proc IEEE 2016;104(5):1058–70.

[2] Castro JR, Saad M, Lefebvre S, Asber D, Lenoir L. Coordinated voltage control in distribution network with the presence of DGs and variable loads using Pareto and fuzzy logic. Energies 2016;9(2):107.

[3] Mo H, Sansavini G. Impact of aging and performance degradation on the operational costs of distributed generation systems. Renew Energy 2019;145:426–39.

[4] Ahmed EM, Mohamed EA, Selim A, Aly M, Alsadi A, Alhosaini W, et al. Improving load frequency control performance in interconnected power systems with a new optimal high degree of freedom cascaded FOTPID-TIDF controller. Ain Shams Eng J 2023;14(10):102207.

[5] Su H-Y, Kang F-M, Liu C-W. Transmission grid secondary voltage control method using PMU data. IEEE Trans Smart Grid 2016;9(4):2908–17.

[6] Kundur P, Paserba J, Ajjarapu V, Andersson G, Bose A, Canizares C, et al. Definition and classification of power system stability. IEEE Trans Power Syst 2004;19(2):1387–401.

[7] Saidi AS. Impact of grid-tied photovoltaic systems on voltage stability of Tunisian distribution networks using dynamic reactive power control. Ain Shams Eng J 2022;13(2):101537.

[8] Sanni MT, Pota H, Mo H, Dong D. Voltage-violation mitigation in power system networks with photo-voltaic penetration. In: 2020 IEEE symposium series on computational intelligence (SSCI); 2020. p. 882–8.

[9] Malachi Y, Singer S. A genetic algorithm for the corrective control of voltage and reactive power. IEEE Trans Power Syst 2006;21(1):295–300.

[10] Hu B, Cañizares CA, Liu M. Secondary and tertiary voltage regulation based on optimal power flows. In: 2010 IREP symposium bulk power system dynamics and control-VIII (IREP). IEEE; 2010. p. 1–6.

[11] Yan W, Cui W, Lee W-J, Yu J, Zhao X. Pilot-bus-centered automatic voltage control with high penetration level of wind generation. IEEE Trans Ind Appl 2015;52(3):1962–9.

[12] Fayek HH, Davis KR, Ghany AA, Abdalla OH. Configuration of WAMS and pilot bus selection for secondary voltage control in the Egyptian grid. In: 2018 North American power symposium (NAPS). IEEE; 2018. p. 1–6.

[13] Yang X, Yang Q, Du Y, Sun L, Deng W. Hierarchical voltage control strategy in multi-bus islanded microgrid based on secondary voltage control bus selection method. J Electr Eng Technol 2021:1–11.

[14] Su H-Y, Chen Y-C, Hsu Y-L. A synchrophasor based optimal voltage control scheme with successive voltage stability margin improvement. Appl Sci 2016;6(1):14.

[15] Abou Daher N, Mougharbel I, Saad M, Kanaan HY, Asber D. Pilot buses selection based on reduced Jacobian matrix. In: 2015 IEEE international conference on smart energy grid engineering (SEGE). IEEE; 2015. p. 1–7.

[16] Sun H, Guo Q, Zhang B, Wu W, Wang B. An adaptive zone-division-based automatic voltage control system with applications in China. IEEE Trans Power Syst 2012;28(2):1816–28.

[17] Di Fazio AR, Russo M, De Santis M. Zoning evaluation for voltage control in smart distribution networks. In: 2018 IEEE international conference on environment and electrical engineering and 2018 IEEE industrial and commercial power systems Europe (EEEIC/I&CPS Europe). IEEE; 2018. p. 1–6.

[18] Dai J, Tang Y, Liu Y, Ning J, Wang Q, Zhu N, et al. Optimal configuration of distributed power flow controller to enhance system loadability via mixed integer linear programming. J Mod Power Syst Clean Energy 2019;7(6):1484–94.

[19] Maharjan R, Kamalasadan S. Secondary voltage control of power grid using voltage stability index and voltage control areas. In: 2017 North American power symposium (NAPS). IEEE; 2017. p. 1–6.

[20] Ilic-Spong M, Christensen J, Eichorn K. Secondary voltage control using pilot point information. IEEE Trans Power Syst 1988;3(2):660–8.

[21] Di Fazio AR, Russo M, Valeri S, De Santis M. Linear method for steady-state analysis of radial distribution systems. Int J Electr Power Energy Syst 2018;99:744–55.

[22] Abou Daher N, Mougharbel I, Saad M, Kanaan HY. Pilot buses selection used in secondary voltage control. In: International conference on renewable energies for developing countries 2014. IEEE; 2014. p. 69–74.

[23] Conejo A, Gomez T, De la Fuente J. Pilot-bus selection for secondary voltage control. Eur Trans Electr Power 1993;3(5):359–66.

[24] Richardot O, Besanger Y, Radu D, Hadjsaid N. Optimal location of pilot buses by a genetic algorithm approach for a coordinated voltage control in distribution systems. In: 2009 IEEE Bucharest PowerTech. IEEE; 2009. p. 1–7.

[25] Amraee T, Ranjbar A, Feuillet R. Immune-based selection of pilot nodes for secondary voltage control. Eur Trans Electr Power 2010;20(7):938–51.

[26] Amraee T, Soroudi A, Ranjbar A. Probabilistic determination of pilot points for zonal voltage control. IET Gener Transm Distrib 2012;6(1):1–10.

[27] Su H-Y, Hong H-H. A stochastic multi-objective approach to pilot bus selection for secondary voltage regulation. IEEE Trans Power Syst 2020;35(4):3262–5.
[28] Xu J, Liu B, Mo H, Dong D. Bayesian adversarial multi-node bandit for optimal smart grid protection against cyber attacks. Automatica 2021;128:109551.
[29] Xu J, Sun Q, Mo H, Dong D. Online routing for smart electricity network under hybrid uncertainty. Automatica 2022;145:110538.
[30] Tatikayala VK, Dixit S. Multi-stage voltage control in high photovoltaic based distributed generation penetrated distribution system considering smart inverter reactive power capability. Ain Shams Eng J 2023:102265.
[31] Bidgoli HS, Van Cutsem T. Combined local and centralized voltage control in active distribution networks. IEEE Trans Power Syst 2017;33(2):1374–84.
[32] Weckx S, Gonzalez C, Driesen J. Combined central and local active and reactive power control of pv inverters. IEEE Trans Sustain Energy 2014;5(3):776–84.
[33] Sahli Z, Hamouda A, Bekrar A, Trentesaux D. Reactive power dispatch optimization with voltage profile improvement using an efficient hybrid algorithm. Energies 2018;11(8):2134.
[34] Liu J-H, Cheng J-S. Online voltage security enhancement using voltage sensitivity-based coherent reactive power control in multi-area wind power generation systems. IEEE Trans Power Syst 2021;36(3):2729–32. https://doi.org/10.1109/TPWRS.2021.3053139.
[35] Abou El Ela A, Abido M, Spea S. Differential evolution algorithm for optimal reactive power dispatch. Electr Power Syst Res 2011;81(2):458–64.
[36] Storn R, Price K. Differential evolution–a simple and efficient heuristic for global optimization over continuous spaces. J Glob Optim 1997;11(4):341–59.
[37] Dong D, Xing X, Ma H, Chen C, Liu Z, Rabitz H. Learning-based quantum robust control: algorithm, applications, and experiments. IEEE Trans Cybern 2019;50(8):3581–93.
[38] Gholizadeh A, Rabiee A, Fadaeinedjad R. A scenario-based voltage stability constrained planning model for integration of large-scale wind farms. Int J Electr Power Energy Syst 2019;105:564–80.
[39] Margellos K, Goulart P, Lygeros J. On the road between robust optimization and the scenario approach for chance constrained optimization problems. IEEE Trans Autom Control 2014;59(8):2258–63.
[40] Jalali A, Aldeen M. Risk-based stochastic allocation of ESS to ensure voltage stability margin for distribution systems. IEEE Trans Power Syst 2018;34(2):1264–77.
[41] Griffone A, Mazza A, Chicco G. Applications of clustering techniques to the definition of the bidding zones. In: 2019 54th international universities power engineering conference (UPEC). IEEE; 2019. p. 1–6.
[42] Global solar irradiance data and pv system power output data. https://solcast.com/. [Accessed 11 June 2021]; 2019.
[43] Zeb MZ, Imran K, Khattak A, Janjua AK, Pal A, Nadeem M, et al. Optimal placement of electric vehicle charging stations in the active distribution network. IEEE Access 2020;8:68124–34. https://doi.org/10.1109/ACCESS.2020.2984127.
[44] Pineda S, Conejo A. Scenario reduction for risk-averse electricity trading. IET Gener Transm Distrib 2010;4(6):694–705.
[45] Heitsch H, Römisch W. Scenario reduction algorithms in stochastic programming. Comput Optim Appl 2003;24(2):187–206.
[46] Resources. https://site.ieee.org/pes-testfeeders/resources/. [Accessed 11 January 2021]; 2021.
[47] Milano F, Vanfretti L. State of the art and future of OSS for power systems. In: 2009 IEEE power & energy society general meeting. IEEE; 2009. p. 1–7.
[48] Zimmerman RD. AC power flows, generalized OPF costs and their derivatives using complex matrix notation. MATPOWER Tech Note 2010;2:60–2.
[49] Di Fazio AR, Russo M, De Santis M. Zoning evaluation for voltage optimization in distribution networks with distributed energy resources. Energies 2019;12(3):390.